The Vertical Temperature Distribution in the Martian Atmosphere

GEORGE OHRING AND JOSEPH MARIANO
GCA Corporation, Bedford, Mass.

19 July 1965 and 25 October 1965

1. Introduction

Previous calculations of the vertical temperature distribution in the Martian atmosphere, based upon a convective-radiative equilibrium model, have been performed by Goody (1957), Ohring (1963), and, most recently, by Prabhakara and Hogan (1965). The two earlier studies were based upon an atmospheric model in which the carbon dioxide content was 2 per cent by volume and the surface pressure was 85 mb. The observations of Kaplan *et al.* (1964) indicate higher carbon dioxide amounts and lower surface pressures than previously observed. These new observations were used in the atmospheric model of Prabhakara and Hogan (1965) and also form the basis for the computations of the vertical temperature profile reported in this note.

2. Theoretical formulation

It is assumed that the most important processes controlling the vertical temperature profile in the Martian atmosphere are radiation and convection. If information is available on the composition of a planetary atmosphere, it is possible to determine the radiative equilibrium temperature profile for that atmosphere. For an atmosphere such as that for Mars or Earth, the radiative equilibrium profile is characterized by superadiabatic lapse rates in the lowest layers. Such a temperature distribution is not stable; in the real atmosphere convection takes place and modifies such a temperature distribution. The effect of convection is to produce a convective-equilibrium lapse rate in the lower layers of the atmosphere. In the earth's atmosphere, in which water vapor condensation takes place, the lapse rate that is established in the lower layers is closer to the moist adiabatic than to the dry. In the Martian atmosphere, in which water vapor is scarce, the lapse rate that is established may be close to dry adiabatic. It is possible to account for this effect of convection in theoretical calculations of the vertical temperature distribution. Rather than computing a pure radiative equilibrium temperature profile, one computes a temperature profile that is characterized by two layers, a lower layer or troposphere in which the lapse rate is equal to the convective lapse rate, and an upper layer or stratosphere that is in radiative equilibrium and in which the lapse rate is stable.

The concepts discussed above can be carried out as follows. Starting with an initial isothermal atmosphere

whose temperature is equal to the average Martian surface temperature, one computes the radiational temperature change rates as a function of altitude. These rates are then applied to the initial temperature profile for a unit time step to obtain a new temperature profile. This process is continued until a temperature profile is obtained for which the radiational rates of temperature change are negligibly small. (In the the present study, a cut-off value of 0.05C day^{-1} is used.) At each stage of the calculations, however, the temperature profiles are checked for instability; if any layer has a lapse rate greater than the convective lapse rate, the temperatures are brought back to the convective lapse rate prior to the next calculation of radiational rates of temperature change. Throughout the computations, the surface temperature is held constant.

3. Physical models

To compute the temperature distribution, a physical model of the atmosphere is required. This model specifies the amounts of absorbing gases, pressure, surface temperature, tropospheric lapse rate, gravitational acceleration, and thermodynamic constants. To evaluate the effect of uncertainties in these parameters, computations were performed for a number of different models. These models are summarized in Table 1, where p_g is the surface pressure, u_{CO_2} is the carbon dioxide abundance, u_{H_2O} is the precipitable water content, the tropospheric lapse rate specifies the lapse rate assumed in the troposphere, c_p is the specific heat of the atmosphere at constant pressure, and T_g is the assumed surface temperature. In all models, nitrogen is assumed to be the only other constituent of the atmosphere. Except for Model 2, which is based upon the previous estimates of surface pressure and carbon dioxide amount, the assumed surface pressures, carbon dioxide amounts, and water vapor amounts are based upon the observations of Kaplan *et al.* (1964). A tropospheric lapse rate equal to the adiabatic lapse rate is assumed for all models except Model 7, where a tropospheric lapse rate equal to 0.65 of adiabatic is assumed. In Models 1–8, the effects of absorption of solar radiation are neglected; in Models 9–11, absorption of solar radiation by the near-infrared bands of carbon dioxide and water vapor is included. In all models, infrared cooling due to water vapor is neglected (a sample calculation comparing carbon dioxide and water vapor infrared cooling rates indicates that this is a reasonable assumption), and the 15 μ carbon dioxide band is assumed to be the only active infrared absorption band. Models 1–4 are designed to test the effects of different surface pressure and carbon dioxide combinations; Models 5 and 6 test the effects of different assumed surface temperatures; Model 7 examines the effect of a subadiabatic lapse rate in the troposphere; and Model 8 examines the effect of a vertical distribution of carbon dioxide in which the carbon dioxide mixing ratio decreases with height. Models 9–11 examine the effects on the computed temperature profile of absorption of solar radiation by carbon dioxide and varying amounts of water vapor.

TABLE 1. Physical models used in computations of vertical temperature distribution.

Model number	p_g (mb)	u_{CO_2} (m STP)	u_{H_2O} (prec. cm)	Tropospheric lapse rate	c_p (cal gm^{-1} deg^{-1})	T_g (°K)
Models in which solar heating is neglected						
1	25	55	0	Adiabatic	0.237	230
2	85	36	0	Adiabatic	0.247	230
3	40	41	0	Adiabatic	0.243	230
4	10	83	0	Adiabatic	0.205	230
5	25	55	0	Adiabatic	0.237	200
6	25	55	0	Adiabatic	0.240	300
7	25	55	0	(0.65)Adiabatic	0.237	230
8	25	55*	0	Adiabatic	0.237	230
Models in which solar heating is included						
9	25	55	0	Adiabatic	0.237	230
10	25	55	10^{-3}	Adiabatic	0.237	230
11	25	55	10^{-2}	Adiabatic	0.237	230

* In this model, the CO_2 mixing ratio decreases by one order of magnitude from the lowest atmospheric layer to the highest layer.

The physical models used in the present study differ in several respects from those assumed by Prabhakara and Hogan (1965). The most important of these are:

a) Prabhakara and Hogan (1965) include the effect of absorption of solar radiation by ozone and oxygen. Ozone and oxygen have not been detected in the Martian atmosphere. If they are present, it is only in very small amounts where both the amounts and vertical distribution of these gases are unknown. Therefore, it was decided not to include them in these computations.

b) The effect of absorption of solar radiation by water vapor is included here, but not in the study of Prabhakara and Hogan.

c) A model with a subadiabatic lapse rate in the troposphere is included here.

d) A model in which the carbon dioxide mixing ratio varies with height is included here.

e) A somewhat wider range of surface temperatures (200 to 300K as opposed to 230 to 270K) is covered here.

4. Computational techniques

Infrared cooling rates are determined from the divergence of the net flux of infrared radiation with height, as computed with the aid of Elsasser's (1960) carbon dioxide radiation tables. For the present computations, these tables have been extended to lower temperatures using procedures outlined by Elsasser (1960). The atmosphere is divided into 20 layers of constant pressure thickness and the upward and downward

fluxes of infrared radiation at the interfaces between layers are computed by numerical integration of the radiative transfer equations. The radiational rate of temperature change is then obtained from

$$\frac{\Delta T}{\Delta t}=\frac{g}{c_p}\frac{\Delta F_{\text{net}}}{\Delta p},$$

where $\Delta T/\Delta t$ is the radiational rate of temperature change for a layer of pressure thickness Δp, g is the acceleration of gravity, and c_p is the specific heat of the atmosphere at constant pressure. Discussions of the details of the computations are presented in Ohring and Mariano (1965) and Ohring (1963).

Except for some minor modifications, heating rates in each layer due to absorption of solar radiation by the near infrared bands of carbon dioxide and water vapor are computed using the method of Roach (1961), which is based upon the experimental absorption data of Howard *et al.* (1955). The heating rate at the mid-point of a layer is determined from

$$\frac{dT}{dt}=\frac{g}{c_p}\cos\psi\sum_i I_{0_i}\frac{dA_i}{dp},$$

where I_{0_i} is the planetary average intensity of solar radiation per wave number at the top of the atmosphere in the i^{th} absorption band, ψ is the planetary average value of the solar zenith angle (60°), A_i is the absorptivity per wave number of the i^{th} absorption band for the atmospheric column extending from the top of the atmosphere to the mid-point of the layer along a slant path parallel to the solar beam, and the summation extends over the near infrared absorption bands of carbon dioxide and water vapor. A discussion of the details of such computations may be found in Roach (1961) and Ohring and Mariano (1965).

The computational methods used here differ from those of Prabhakara and Hogan (1965). The major differences are:

a) In their radiative transfer equations, Prabhakara and Hogan use transmission functions for carbon dioxide that are theoretically calculated with the use of a statistical model for band absorption. The present calculations make use of Elsasser's (1960) radiation tables, in which the infrared transmission functions are determined empirically from laboratory absorption data, and Roach's (1961) technique, which is also based upon laboratory absorption data.

b) Prabhakara and Hogan obtained their final temperature distribution by essentially solving a series of simultaneous equations with the use of an iterative scheme. In the present study, the final temperature distribution is obtained, as discussed above, by essentially approaching an asymptotic steady state for an initial value problem. This method has also been called the time-marching method.

5. Results

The computed temperature profiles are shown in Fig. 1, with the ratio of pressure to surface pressure and height as the vertical coordinates. The height of the computed tropopause—the boundary between the lower convective zone and upper radiative equilibrium zone—is indicated by a short horizontal bar. The number for each temperature profile refers to the physical model used in the calculation. Profiles 1–4, which cover a range of surface pressures from 10 mb to 85 mb and the carbon dioxide amounts associated with these pressures are remarkably similar. The average temperature in the highest layer is about 127K, and all four profiles fall within 2K of this value. The height of the tropopause is about 7 km for all four profiles. Temperature profile 1, the 25-mb case, may be compared to a similar profile computed by Prabhakara and Hogan (1965) for a 30-mb case (Fig. 4 of their paper; curve labeled radiative-convective). The computed height of the tropopause is about the same in both calculations, but our temperatures above 20 km are some 15–20K lower than those of Prabhakara and Hogan.

Temperature profiles 5 and 6 illustrate the effect of changing the assumed surface temperature. As the surface temperature changes from 200K to 300K, the height of the tropopause increases. The two profiles tend to converge at upper levels, thus resulting in a smaller difference in temperature at upper levels than at the surface. The calculations of Prabhakara and Hogan (1965) indicate a similar tendency.

The effect of a tropospheric lapse rate equal to 0.65 of the adiabatic lapse rate is shown by profile 7. The tropopause height is considerably increased, but the overall difference between this profile and profiles 1–4 is relatively small.

The effect of a non-uniform distribution of carbon dioxide is shown in profile 8, which is for a model in which the carbon dioxide mixing ratio decreases linearly from the lowest layer to the highest layer by one order of magnitude. This profile is characterized by a high and relatively sharp tropopause.

Temperature profiles 9, 10, and 11 represent the effects of a step-wise introduction of solar heating. Profile 9 is based upon a model that includes only carbon dioxide heating; profile 10 includes heating due to carbon dioxide and 10^{-3} prec. cm of water vapor [a value consistent with the observations of Kaplan *et al.* (1964)]; and profile 11 includes heating due to carbon dioxide and 10^{-2} prec. cm of water vapor (a possible upper limit for the amount of water vapor). Inclusion of carbon dioxide heating raises the upper level temperatures about 17K; with the addition of water vapor heating, the upper level temperatures are

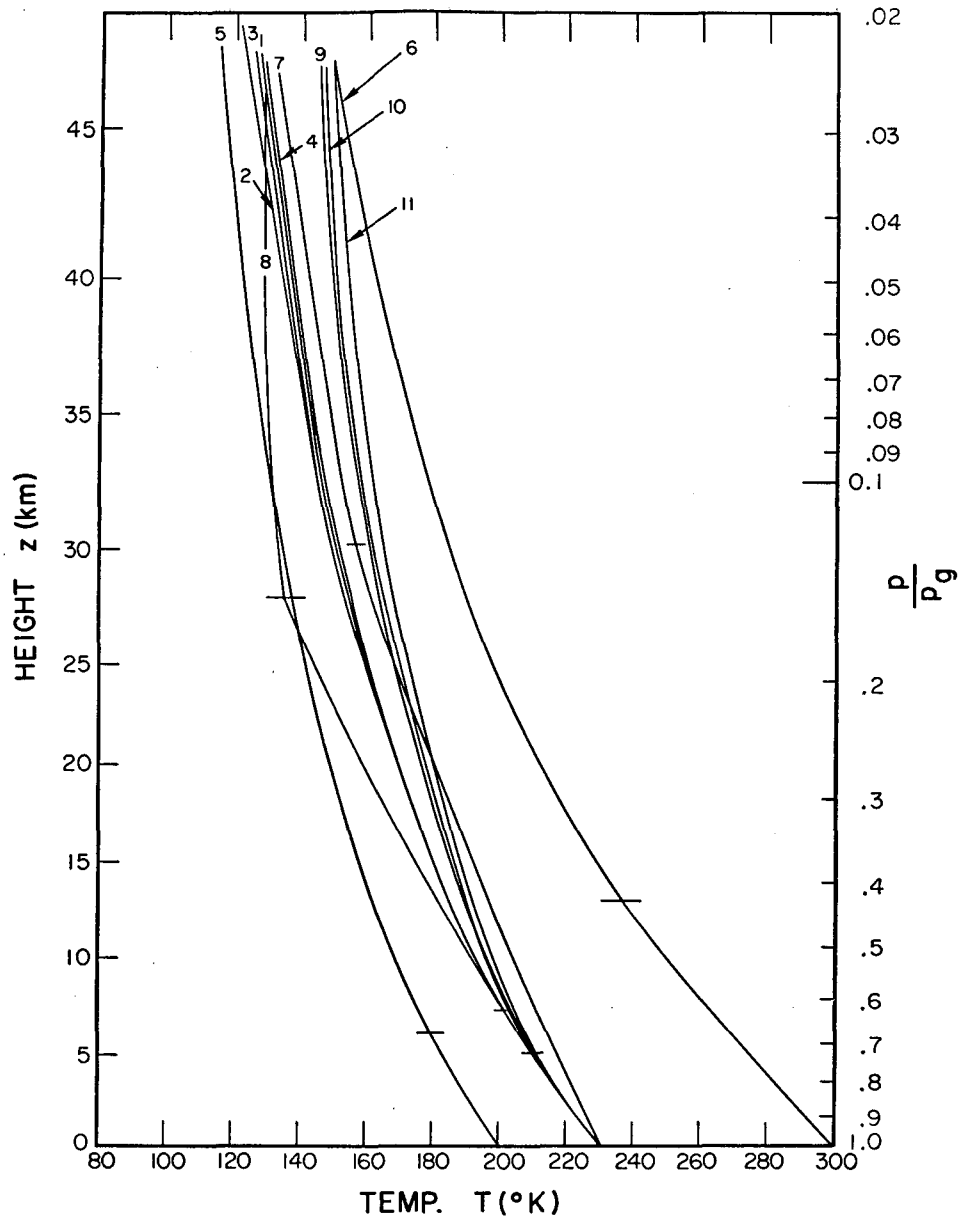

FIG. 1. Vertical distributions of temperature in the Martian atmosphere for all physical models.

further increased by several degrees. The solar heating models of Prabhakara and Hogan (1965), which include carbon dioxide, ozone and oxygen, but not water vapor, also indicate a temperature increase at upper levels of about 20K over a model that neglects solar heating. Inclusion of solar heating tends to lower the tropopause by about 2 km, an effect also indicated by the results of Prabhakara and Hogan.

6. Summary

Vertical temperature distributions computed for the Martian atmosphere indicate that the temperatures are not sensitive to variations in surface pressure and carbon dioxide comparable to present uncertainties in these parameters, a result also evident in the computations of Prabhakara and Hogan (1965). Where comparisons could be made between the present results and those of Prabhakara and Hogan, they indicate that the computed temperature profiles are in good qualitative agreement but that the present profiles are some 15–20K lower above 20 km.

Acknowledgments. This research was supported by the National Aeronautics and Space Administration, Manned Spacecraft Center, under Contract NAS9-3423.

REFERENCES

Elsasser, W. M., 1960: Atmospheric radiation tables. *Meteor. Monogr.*, 4, No. 23, 43 pp.

Goody, R., 1957: The atmosphere of Mars. *Weather*, 12, 3–15.

Howard, J. N., D. L. Burch and D. Williams, 1955: Near infrared transmission through synthetic atmospheres. AFCRC *Geophys. Res. Papers*, No. 40 (ASTIA AD-87679), 244 pp.

Kaplan, L. D., G. Munch and H. Spinrad, 1964: An analysis of the spectrum of Mars. *Astrophys. J.*, 139, 1–15.

Ohring, G., 1963: A theoretical estimate of the average vertical distribution of temperature in the Martian atmosphere. *Icarus*, 1, 328–333.

——, and J. Mariano, 1965: Study of the average vertical distribution of temperature in the Martian atmosphere. Final Report, NASA Contract NAS9-3423, GCA Technical Report 65-3-N, 76 pp.

Prabhakara, C., and J. S. Hogan, 1965: Ozone and carbon dioxide heating in the Martian atmosphere. *J. Atmos. Sci.*, 22, 97–109.

Roach, W. T., 1961: The absorption of solar radiation by water vapor and carbon dioxide in a cloudless atmosphere. *Quart. J. R. Meteor. Soc.*, 87, 364–373.